www.rericjournal.ait.ac.th

Numerical Study of PCM Melting Effects in Fin Type Rectangular Encapsulation Incorporating Aluminum Spiral Fillers

L. Tan*[1], Y. Kwok, A. Date, and A. Akbarzedah

Abstract – *A numerical investigation was carried out to understand the melting characteristics of PCM in an internal fin type rectangular encapsulation with the addition of aluminum spiral fillers. Increasing the number of fins in PCM thermal storage encapsulation can significantly improve melting performance but to some values where only lead to marginal improvement in heat transfer rate. Adding aluminum spiral fillers within the fin gap can be an option to improve heat transfer internally. This paper presents extensive computational visualizations on the PCM melting patterns of the proposed fin-spiral fillers configuration in a four fins rectangular encapsulation. The aim of this investigation is to understand the PCM's melting behaviors by observing the natural convection currents movement and melting fronts formation. Fluent 6.3 simulation software was utilized in producing two-dimensional visualizations of melting fractions, temperature distributions and flow fields to illustrate the melting process internally. The results have shown that with the present of aluminum spiral fillers in fin-type slab have better melting rate than pure fin type slab. Greater liquid regions are observed internally which promoted more active natural convection currents and improved melting performance.*

Keywords – Fins, metallic spiral fillers, paraffin wax, phase change material, thermal enhancement.

1. INTRODUCTION

PCM thermal storage or latent heat storage system plays important roles in energy conservation for environmental and civil engineering. Designing an effective thermal storage system is able to reduce the mismatch between supply and demand of energy. Solar heating system is one of the examples used in civil engineering where PCM thermal storage tanks are utilized for storing thermal energy dissipated by the sun in day time and reuse the stored heat for thermal condition such as air and water supply in buildings. Thermal storage systems are also capable to keep hot water for a longer period in water tanks at designated temperature and duration where it can be easily sized by selecting the desired type and amount of the PCM used in the thermal storage systems.

Latent heat storage has higher heat storage density than sensible heat storage due to the present of latent heat of fusion of which material undergoing phase change. For instance, typical rock-based sensible heat storage requires seven times of storage mass compared to paraffin 116 wax for storing the same amount of heat energy [1]-[2]. It also possesses isothermal or near isothermal operation depending on the purity of the PCM used in the system. Because of this high heat capacity capability, this technology is further exploited in electronics cooling where PCMs are used for regulating the operating temperature of the electronic devices [3].

Despite the fact that latent heat storage serves as high thermal energy density and process near isothermal operation, sensible heat method is still the preferred method for thermal storage system design. The main issue on using latent heat method lies on the poor thermal conductivity of the PCM which limits the rate of heat absorbing and releasing. Commercial paraffin waxes are cheap and delivered acceptably high heat storage density (~200 kJ) with wide range of melting temperatures. They are also chemically stable, high thermal cyclic and no phase segregation which make them ideal PCM in the thermal storage system. However, the low thermal conductivity (~0.2W/m K) has greatly limited their potentials and applications. Despite inorganic salt hydrates have higher thermal conductivity (~0.5W/m K) and energy density (~450KJ/kg), phase segregation and super cooling are negative factors in thermal storage design. To embark on economical and feasible storage system, degradation of PCM and corrosion of storage tank are important factors to be considered. Hence, improving the thermal conductivity of organic PCM will still be a prospective direction for future latent heat storage development. Without having a simple solution on improving heat transfer performance, this technology will still remain as unsuccessful for large scale applications and also be restricted on higher heat flux applications. Published literatures [4]-[5] have reviewed on various thermal enhancement methods for improving the heat transfer performance of latent heat storage systems. These approaches are: using extended surface (fins), employing multiple PCM's method, metal matrix, metallic fillers and micro-encapsulation. In this present investigation, extending surface using fins as thermal enhancement method will be discussed in detailed.

Extending heat transfer surface using internal fins in thermal storage is one of the simple and effective approaches for improving the melting rate of PCM in the thermal storage. However, the increasing number of

*Energy Conservation and Renewable Energy Group, RMIT University, Bundoora East Campus, Melbourne, Australia.

[1]Corresponding author;
E-mail: lippong.tan@rmit.edu.au

internal fins will only increase the effective thermal conductivity and not contribute to a sharp increase in the overall heat transfer coefficient. This is because natural convection heat transfer effect is diminished within the smaller fin gap volume. Gharebagi and Sezai [6] had investigated the performance of rectangular PCM device with horizontal fins added to heated vertical walls. They found out that with the increasing of fins only leaded to a marginal increase in heat transfer rate. Thus, concluded that increasing number of fin will hamper the effect of natural convection within the system and melting would become a conduction-dominated process. In regard to the natural convection effect in a small volumetric PCM enclosure, the authors shared similar observations when experimenting on the melting performance of paraffin wax in 87% porosity honeycomb slab and 4-fins rectangular slab. The unpublished comparative results showed that honeycomb slab with high porosity did not exhibit significant heat transfer rate improvement. It is observed that heat is transferred to the solid PCM by conduction at initial stage and growing layer of liquid PCM is formed near the heating walls and fins at the latter stage. As liquid PCM normally has lower thermal conductivity (~0.15W/m K, tested paraffin wax) than in solid state (~0.2W/m k, tested paraffin wax), heat transfer by conduction will gradually decline with the thickening of the liquid zone, generating a thermal resistance. Thus natural convection heat transfer will be dominant as it is driven by the temperature gradient in the liquid zone and dissipate the heat to the surrounding regions of the solid PCM by buoyancy forces. Lamberg *et al*. [7] had proven the natural convective effect by conducting an experimental and numerical study on melting performance of PCM in a rectangular enclosure, with and without natural convection effect. The results showed that PCM took double the time to reach the maximum temperature when natural convection effect was ignored. Jellouli *et al*. [8] also did an experiment on melting of PCM in rectangular enclosure with heating at the bottom. The isotherms obtained were horizontal at the early stage and became accentuated at the latter stage. Based on this phenomenon, he concluded that conduction dominated melting process at the early stage and gradually shifted to natural convection effect during melting test.

The objective of this work is to investigate numerically on the melting behaviors of adding aluminum spiral fillers into the internal fin type rectangular encapsulation (slab). As mentioned in the literature that increasing number of fins would not experience great improvement in melting, the authors aim to improve the heat transfer performance by optimizing both conduction and natural convection heat transfer effects during melting by adding metallic fillers. Incorporating aluminum spiral fillers in fin slab are expected to promote natural convective effect within the wider fin gap regions and also increase the effective thermal conductivity due to higher aluminum content. In this paper, extensive numerical simulations have been carried out where simulated visualizations are developed for observing the PCM melting effects and patterns. Melt fractions, temperature distributions and flow fields at various heating durations are visually presented.

2. NUMERICAL ANALYSIS

In this section, two different internal configurations of the experimental rectangular slabs filled with PCM are numerically investigated. Commercial simulation software (Fluent 6.3) is used to solve the conservation equations for mass, momentum and energy. A physical model of the system and the computational procedure are presented in detail in this section.

2.1 Experimental Set-up

The main components in the experiment are paraffin wax as PCM and two aluminum rectangular slabs with physical dimensions of 300mm (length) x 300mm (width) x 25mm (depth). Four aluminum fins with thickness of 4mm are installed in rectangular slab (A) and similar 4 fins-type slab are added with aluminum spiral fillers. The container walls have similar thickness and material as the installed aluminum fins. Commercial paraffin wax was used as PCM in the experimental and numerical investigation. In order to understand the specific heat capacity variation over temperature of the PCM during melting, samples of paraffin wax (~10mg) were sent to RMIT chemical department for differential scanning calorimetry (DSC). The DSC scanning results in Figure 2 shows that the peak melting temperature is 47^{o}C with latent heat of ~140kJ/kg. The summarized thermo-physical properties are detailed in Table 1.

A total of nine T-type thermocouples are located at different locations shown in Figure 3 for recording temperatures during phase change process. Thermocouples 1-5 are used for measuring the PCM temperature at different heights during melting. Thermocouple 6 and 7 are used to capture the top (Perspex sheet, 3mm thick) for accounting heat loss and the bottom of aluminum plate. All exposed surface of the slab is fully insulated using glass wools which has a high thermal resistance of ~28^{o}C/W. The heater used is hot plate stirrer (model 209-1) from IEC Pty Ltd and the data acquisition unit is Agilent 34970A for capturing the respective temperature at timely basis.

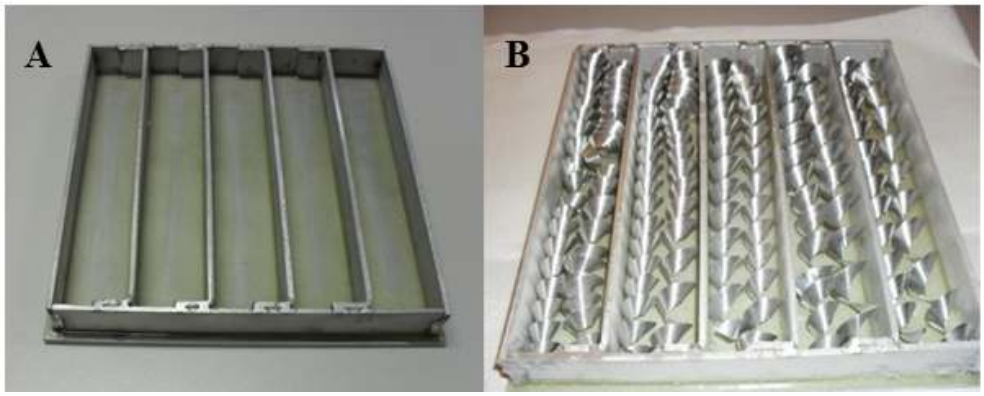

Fig. 1. Experimental PCM slabs: Fin-type (A), fin-spiral fillers (B).

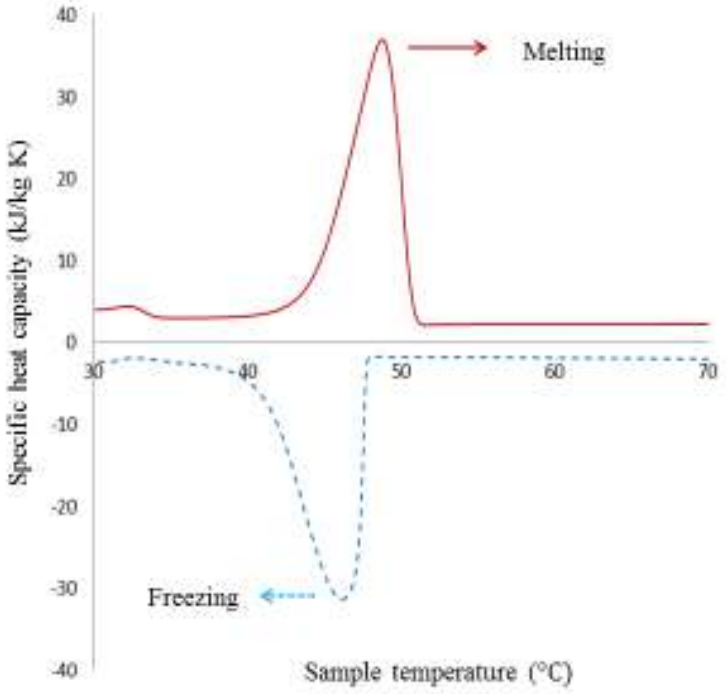

Fig. 2. DSC graphical result for used paraffin wax.

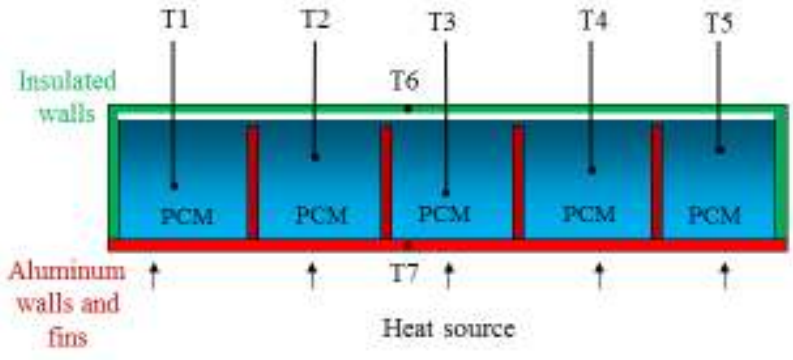

Fig. 3. Schematic diagram for fin-type PCM slab and thermocouple locations.

Table 1. Thermo-physical properties of tested paraffin wax.

Parameters	Values
Density [kg/m^3]	880 (solid)/760 (liquid)
Specific heat [kJ/kg K]	2.9 (solid)/2.2 (liquid)
Thermal conductivity [W/m K]	0.2
Melting temperature [^{o}C]	47
Latent heat [kJ/kg]	140
Thermal expansion [K^{-1}]	0.001

2.2 Physical Model

A schematic 2-D computational domain for fin type and fin-spiral fillers slab are shown in Figures 4 and 6 respectively Due to geometrical symmetry of both rectangular encapsulations, half of the geometry would be used in the modeling for time and memory saving during computation.

All fins are embedded in PCM with a thin air gap between the PCM and insulated wall. It is noted that PCM expands with the increasing temperature, constrained environment will be assumed in this modeling where thin gap of air and thermal expansion are neglected in this case.

Figure 5 shows an aluminum spiral filler strip in the rectangular slab. Due to the geometrical complexity in modeling helical shape, a 2-D circular shape will be used to model aluminum circular wall for simplicity. The mean diameter of the helical shape is be used to represent the spiral filler walls where the circular wall model will be elevated from the bottom plate in this two-dimensional numerical analysis. It is noted that there would be a PCM mass reduction using this simplified method. A volume-corrected version has developed for validation the experimental results.

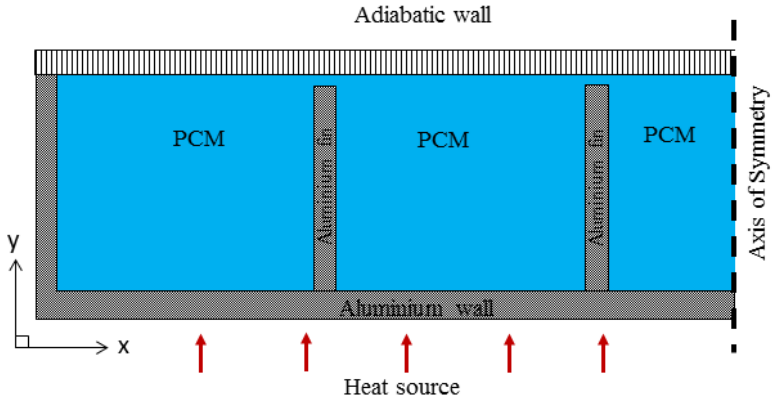

Fig. 4. Computational domain for fin type (4 fins) encapsulation.

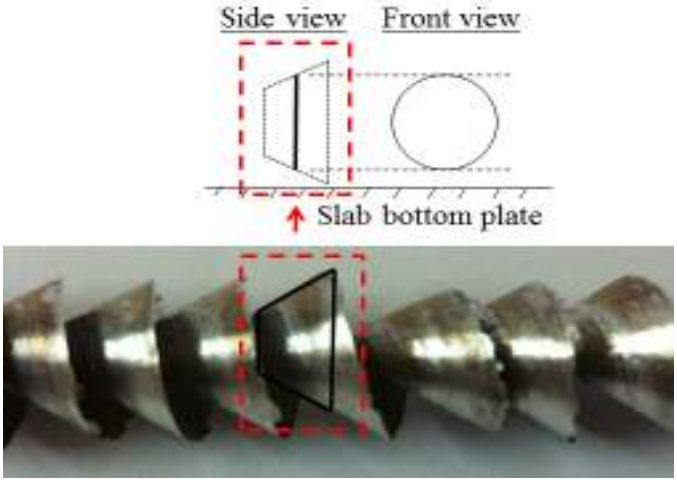

Fig. 5. Simplified computational model for spiral fillers.

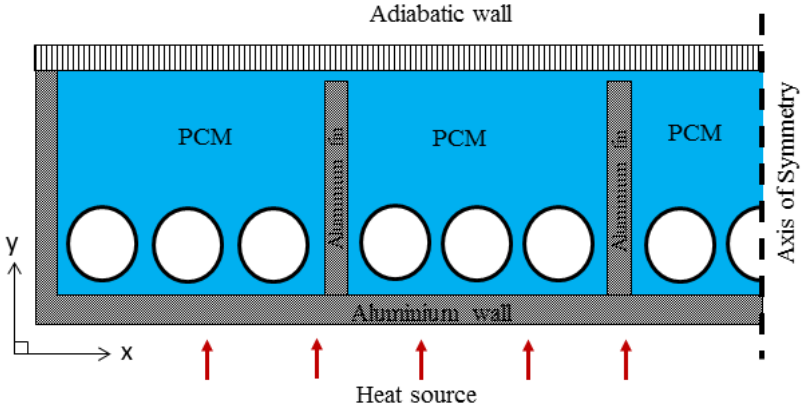

Fig. 6. Computational domain for fin-spiral fillers encapsulation.

Table 2. Material properties assumed in the simulation.

Parameters	Aluminum	PCM
Thermal conductivity (W/m K)	202.4	0.2
Density (kg/m^3)	2719	$880[1-0.001(T-320)]$
Specific heat (J/kg K)	871	2500
Latent heat (kJ/kg)	-	140
Melting temperature (^{o}C)	-	43-49

Constant heat flux of 1000W/m^2 is supplied to the base of the encapsulation. The computation properties of PCM and aluminum are listed in Table 2. Boussineq approximation is adopted to calculate the change in density as a function of temperature in the liquid density given by:

$$\rho = \rho_o\left[1-\beta\left(T-T_m\right)\right] \tag{1}$$

and the relationship of buoyancy forces in the momentum equation is given by:

$$-\rho g = \rho_o g\left[\beta\left(T-T_m\right)-1\right] \tag{2}$$

Where ρ_0 is the reference density at melting temperature T_m, and β is the thermal expansion which valued at 0.001 based on the data provided by Humphries and Griggs [9]. The dynamic viscosity of the liquid PCM is given by [10]:

$$\mu = 0.001\times\exp\left(-4.25+\frac{1790}{T}\right) \tag{3}$$

2.3 Governing Equations

Enthalpy-porosity formulation [7] is adopted in solving phase change region in PCM. Similar set of governing equations used in the computation are given by Shatikian *et al*. [11]:

Continuity:

$$\frac{\partial}{\partial x_i}\left(\rho u_i\right) = 0 \tag{4}$$

Momentum:

$$\frac{\partial}{\partial t}\left(\rho u_i\right)+\frac{\partial}{\partial x_i}\left(\rho u_i u_j\right) = \mu\frac{\partial^2 u_i}{\partial x_i x_j}-\frac{\partial P}{\partial x_i}+\rho g_i+S_i \tag{5}$$

Energy:

$$\frac{\partial}{\partial t}\left(\rho h\right)+\frac{\partial}{\partial x_i}\left(\rho u_i h\right) = \frac{\partial}{\partial x_i}\left(k\frac{\partial T}{\partial x_i}\right) \tag{6}$$

Where ρ is the density, k is the thermal conductivity, μ is the dynamic viscosity, S_i is the momentum source term, u_i is the velocity component, x_i is the Cartesian coordinate and h is the specific enthalpy. The sensible enthalpy h_s is given by:

$$h_s = h_{ref}+\int_{T_{ref}}^{T} C_p dT \tag{7}$$

And the total enthalpy, H is defined as:

$$H = h_s+\Delta H \tag{8}$$

The total enthalpy is the sum of sensible enthalpy h_s and the enthalpy change due to phase change γL, where h_{ref} is the reference enthalpy at the reference temperature T_{ref}, C_p is the specific heat, L is the specific enthalpy of melting (liquid state) and γ is the liquid fraction during the phase change which occur over a range of temperatures $T_s < T < T_l$ defined by the following relations:

$$\gamma = \frac{\Delta H}{L} = 0 \quad \text{if} \quad T_s < T \quad \text{[Solid]} \tag{9}$$

$$\gamma = \frac{\Delta H}{L} = \frac{T - T_s}{T_l - T_s} \quad \text{if } T_s < T < T_l \quad \text{[Mushy]} \qquad (10)$$

$$\gamma = \frac{\Delta H}{L} = 1 \quad \text{if} \quad T > T_l \quad \text{[Liquid]} \qquad (11)$$

The source term S_i in the momentum equation (eqn. 5) is given by:

$$S_i = -A(\gamma)u_i = \frac{C(1-\gamma)^2}{\gamma^3 + \varepsilon} u_i \qquad (12)$$

Where $A(\gamma)$ is defined as the "porosity function" which governed the momentum equation mimic Carman-Kozeny equations for flow in porous media introduced by Brent *et al*. [12]. The function reduces the velocities gradually from a finite value as 1 in fully liquid to 0 in fully solid state within the computational cells involving phase change. The epsilon ε=0.001 infinity avoidance constant due to division by zero and C is a constant reflecting the morphology of the melting front where C = 10^5 is assumed in this study which has been used in by Shatikan *et al*. 11].

2.4 Computational Methodology

The SIMPLE algorithm has been used for solving the mass, momentum and energy governing equations. Approximately about 35,000 triangular and quadrilateral cells were meshed for the two different configurations for solving the flow fields, melt fractions and temperature distributions. The time step selected was 1 second where comparative testing on time step of 0.1, 0.5 and 1 seconds had shown little difference which deemed to be neglected. Hence, larger time step of 1 second can be used for saving computational time. The maximum number of iteration for every time step is between 10 and 20 as recommended by Fluent [13].

3. RESULTS AND DISCUSSIONS

In this section, melting visualizations have been developed and discussed. As the experimental PCM slab prototypes are made of aluminum, melting process is not visible during testing. The developed melting front visualizations will be used as a predictive tool for observing the melting phenomenon.

3.1 Model Validation

Model validation was performed by comparing of the numerically predicted temperature data with experimental data at thermocouple location (T2) showed in Figure 3.

Figures 7 and 8 show the numerical and experimental temperature history comparison at the thermocouple location (T2). The validation showed good agreement between both data over time where both results stayed within 4°C. It is also noted that the fin-spiral fillers configuration is model by using circular aluminum walls which will result lesser PCM volume as compared to fin type configuration. As a result, the numerical model will reach fully liquid earlier, shorter phase change period and higher maximum temperature which is not ideal for validation. To ensure consistency, an additional model, volume-corrected version has developed in the simulation to verify the experiment data with the same amount of PCM filled. As expected, the pre-volume corrected fin-spiral model has shown a quicker rise in temperature and shorter phase change period. The volume-corrected version displayed a good agreement with the experimental results. The objective of this numerical study is to improve melting by observing the melting effects by adding aluminum spiral filler into the designated fin slab. Hence pre-volume corrected fin-spiral fillers will be used in the analysis.

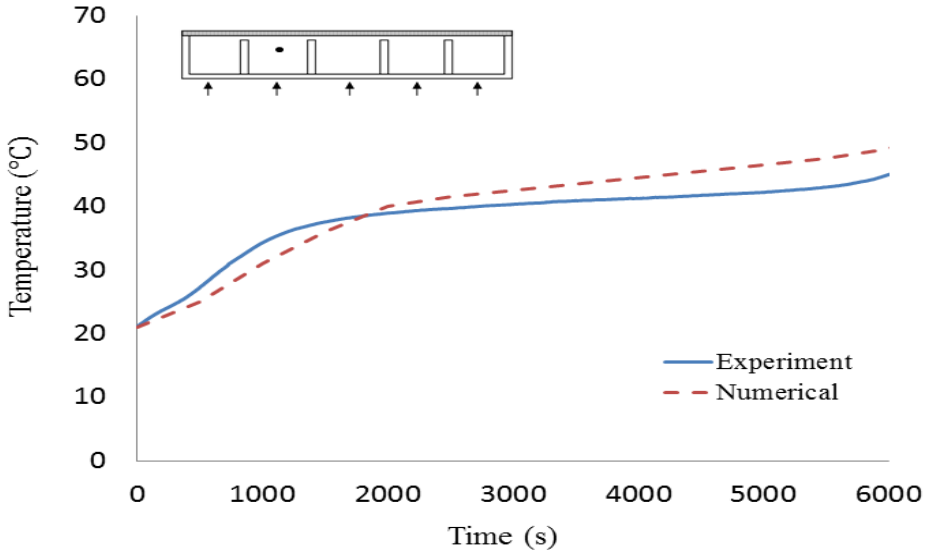

Fig. 7. Numerical and experimental results comparison for fin slab configuration at thermocouple T2.

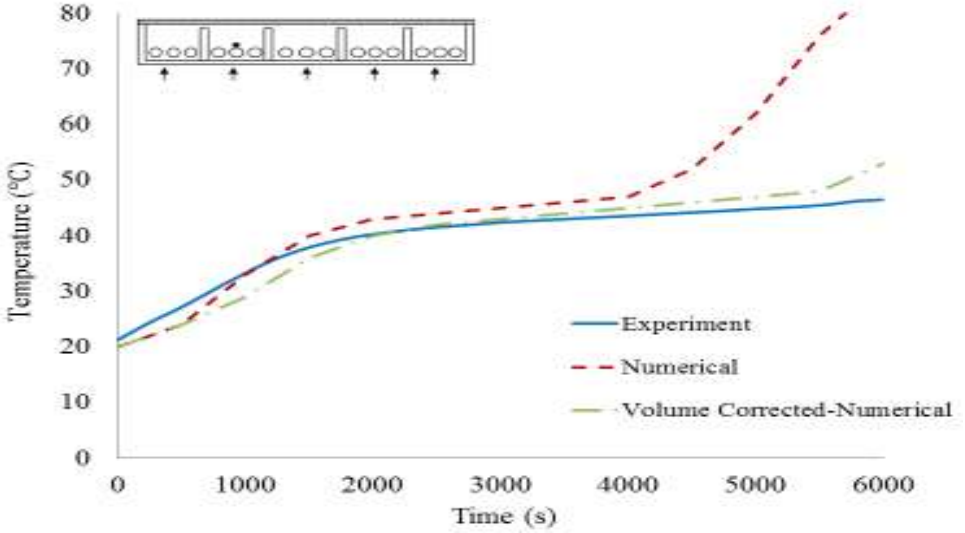

Fig. 8. Numerical and experimental results comparison for fin-spiral fillers slab configuration at thermocouple T2.

3.2 Computational visualization

Figures 9 and 10 present the melt fractions for fin and fin-spiral fillers configurations under 1000W/m^2 of constant heating at the bottom part of the slab. Three different stages of melting: 1800 seconds (30 minutes), 3600 seconds (60 minutes) and 5400 seconds (90 minutes) are used in this analysis.

It is clearly seen that both configurations have the similar melting performance at the first 30 minutes (M-F1 and M-FS1). Melting of PCM is initiated at the wall boundaries by heat conduction in the aluminum walls and fins. It is observed in the fin-spiral fillers configuration that melting front is formed around the metallic wall surfaces and not at the spiral filler walls as heat flow is hindered by the poor thermal conductivity of the PCM present in between. However, there is a small effect present at the bottom melting front. There is a slight increase in the melting front in a wavy fashion formed due to the influence of higher effective thermal conductivity contributed by the aluminum content by the fin-spiral fillers.

As heating continues, the melting behaviors of both configurations became very different in the later stages. At 60 minutes time stage, large portions of liquid fraction are seen forming around the spiral fillers shown in Figure 10 under M-FS2 melt fraction contour. The liquid fraction illustrated in red started to become wider and wavy as compared to fin type slab. This is due to the present natural convection heat transfer in assisting the melting. Fin type slab (M-F2) shown in Figure 9 has a steady melting pattern without any sign of abrupt change in melting fronts. The natural convection effect is weak as smaller liquid PCM circulated around the wall surfaces. As mentioned earlier, density of PCM has a decreasing function with respect to temperature rise in liquid PCM. This will generate buoyancy forces which are driven by temperature difference in dissipating the heat to the other cooler regions of the PCM along the interface.

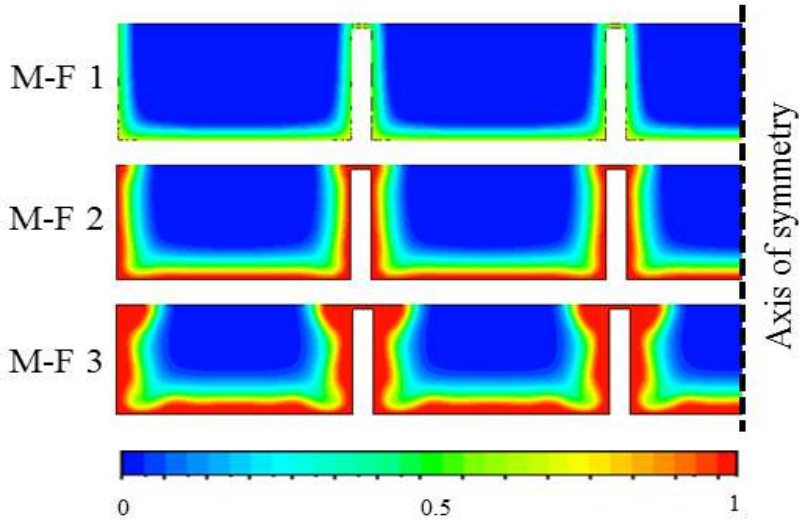

Fig. 9. Melt fraction for fin type (M-F 1/2/3) at 1800, 3600 and 5400 seconds, respectively.

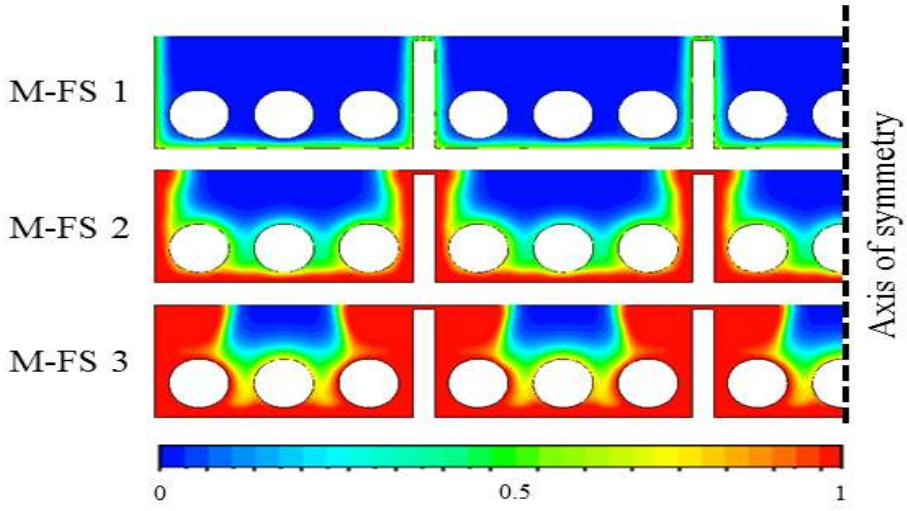

Fig. 10. Melt fraction for fin-spiral fillers (M-FS 1/2/3) at 1800, 3600 and 5400 seconds, respectively.

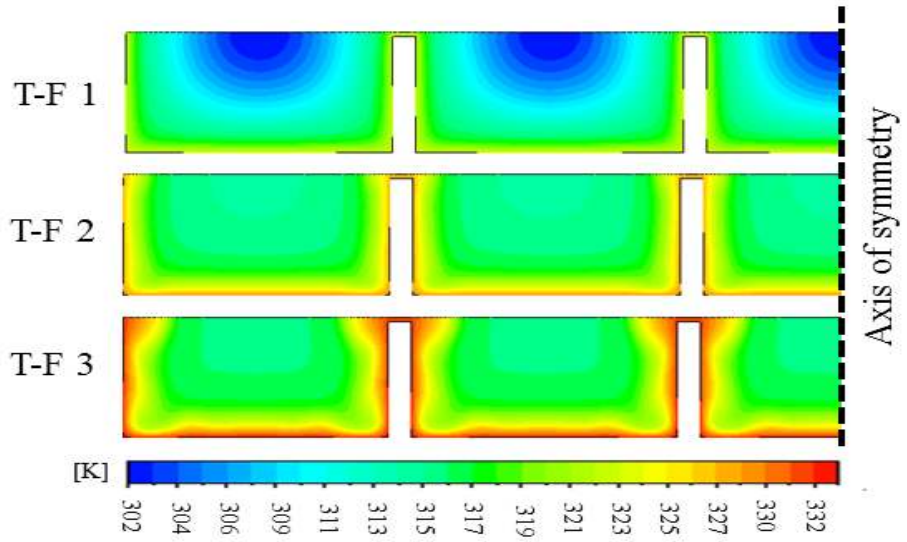

Fig. 11. Temperature distributions of fin type (T-F 1/2/3) at 1800, 3600 and 5400 seconds.

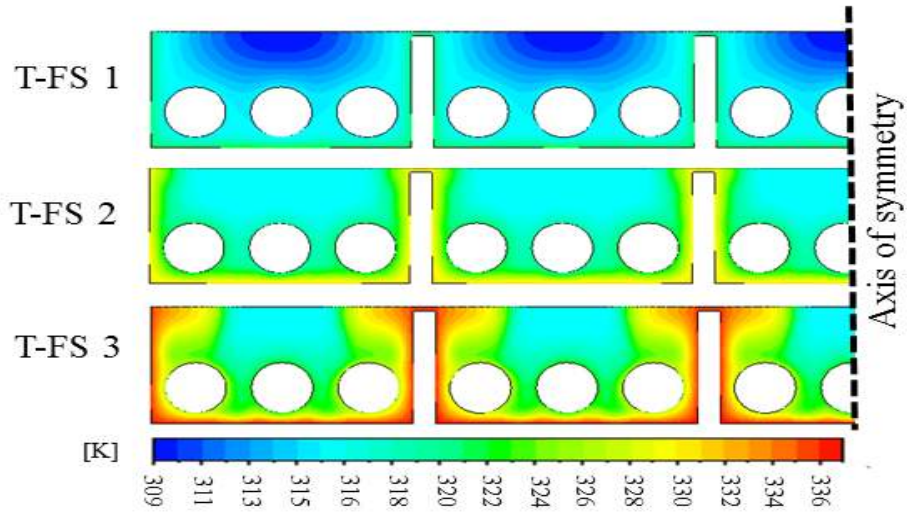

Fig. 12. Temperature distributions of fin-spiral fillers (T-FS 1/2/3) at 1800, 3600 and 5400 seconds.

Figures 11 and 12 show the temperature distributions for both slab configurations at different time stages. It is clearly seen that higher temperature range is present in fin-spiral filler slab compared to fin type slab. This phenomenon shows that the natural convection current played a major role in reducing the thermal resistance of the PCM in the encapsulation.

Figures 13 and 14 show the convective flow fields

for both slab configurations at 60 minutes simulation. The convective flow fields represented in arrows and the contour lines represent the temperature boundaries of the melting PCM. In fin type configuration, there is strong stream of vortices circulating near the fin walls, transfer heat from the hotter bottom region to the top cooler region. This convective heat transfer circulation assisted melting solid-liquid interface near the walls but it still maintained a high thermal resistance in the middle cooler region where heat is not effective penetrated. By adding aluminum spiral fillers will enhance this convective heat transfer effect to the middle region of the PCM. It is seen that there is convective vortices present around the circular wall which would eventually got stronger with greater liquid fraction formation. This is due to the higher thermal conductivity of aluminum spiral filler assisted in expanding more liquid regions at the middle section and resulted more temperature driven vortices for heat dissipation than fin type configuration. In addition, the greater liquid zone provided more natural convection heat transfer effect and created a smaller temperature gradient within fin partition.

There are multiple regions of active convective flow fields propagating in the fin-spiral fillers slab, especially at the spiral fillers regions. This active flow effect will reduce the thermal resistance of the mushy zone by dissipating heat to the cooler region in slab. In fin type slab, the convective flow fields seem to be active around the heated wall region and weaker at the melting interface. Hence, the heat transfer would be less effective as it creates a thermal resistance for the heat to enter into the core of the solid PCM. At 90 minutes, fin type slab experienced a faster melting as evidenced by the greater liquid fraction in red (M-F3). The melting front became wavy caused by the random convective flow effects.

It is noted that the dominance heat transfer in PCM is conduction in solid state and natural convection in liquid state. It is clearly seen that fin-spiral fillers configuration developed greater liquid fraction than fin type over the same period of time. A melt fraction for fin type, fin—spiral filler and volume-corrected fin-spiral fillers configurations are compared and showed in Figure 17.

The melt fraction representation evaluates the melting performance of PCM in different heat enhancement configurations with respect to time. Based on the results shown in Figure 17, by adding spiral fillers has showed which has a direct relationship of melting performance in the respective internal configuration. It took a shorter time to become fully liquid as compared to the fin type configuration. Volume-corrected fin-spiral fillers configuration also showed a faster melting performance with the same amount of PCM filled as compared to fin type configuration.

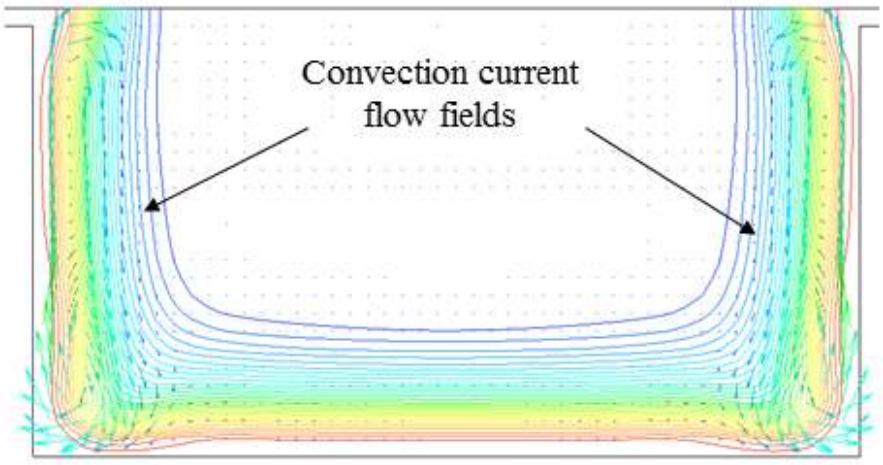

Fig. 13. Convective flow fields of fin type configuration at 3600 seconds.

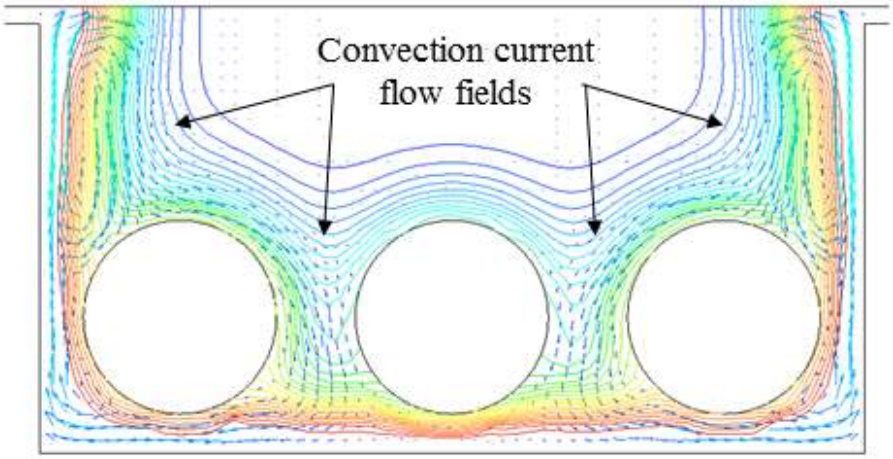

Fig. 14. Convective flow fields of fin-spiral filler configuration at 3600 seconds.

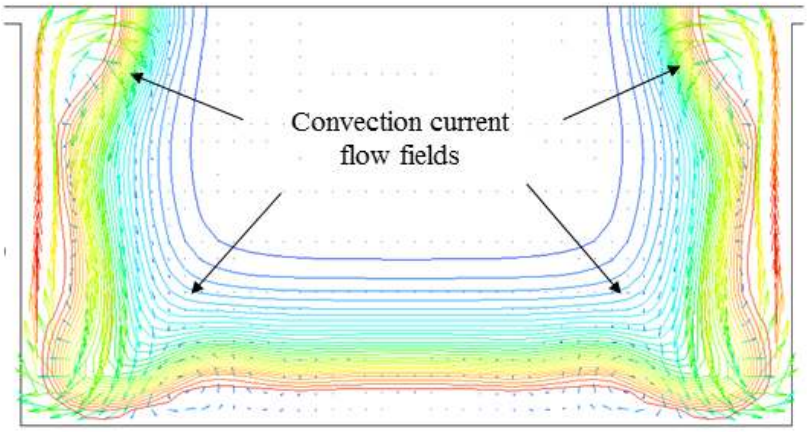

Fig. 15. Convective flow fields of fin type configuration at 5400 seconds.

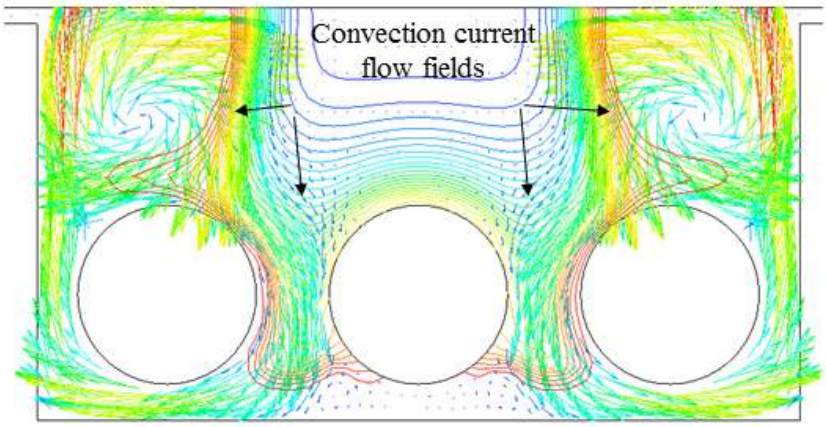

Fig. 16. Convective flow fields of fin-spiral filler configurations at 5400 seconds.

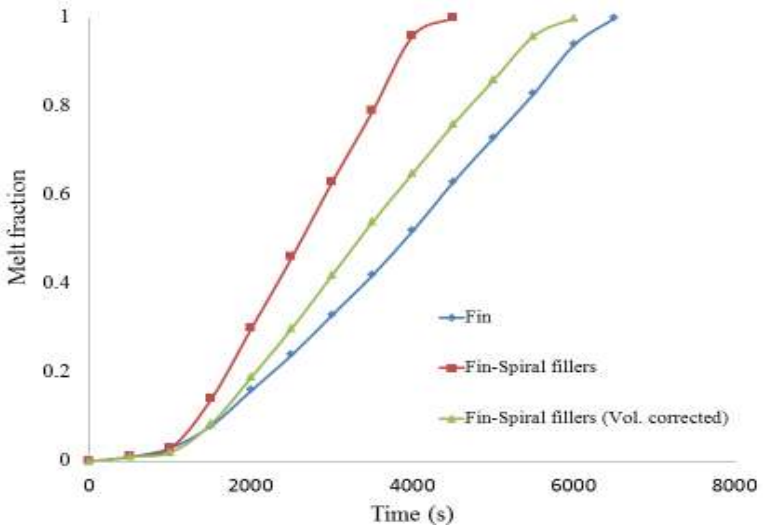

Fig. 17. Numerically predicted melt fraction comparison for fin and fin-spiral fillers configurations.

4. CONCLUSIONS

In this present work, melting performance in fin and fin-spiral fillers configurations has been numerically investigated. The numerically analysis is conducted based on enthalpy-porosity formulation and the simulated results are validated with the experimental data. The numerical validation possessed good agreement with the experimental. The following conclusions are drawn:

- Adding aluminum spiral fillers to inner fin type slab does not have any significant in melting performance in solid state. However, melting rate speed up in the latter stage where spiral fillers promote natural convection effect at melting interfaces and affect the melting pattern from gradual to abrupt wavy melting fronts.
- The visualization of fin-spiral fillers configurations had shown better melting performance than the fin type configuration by promoting more natural convection currents at the middle region near the core of the solid PCM. This would assist melting as more heat is dissipated to the solid PCM by natural convection currents.
- This proposal will be much easier to increase the heat transfer coefficient of the rectangular PCM thermal storage without much manufacturing complexity than increasing the number of fins internally.
- Further research on using smaller and more spiral fillers are recommended for higher melting rate as it is expected to increase the effective thermal conduction and able to generate more natural convective regions within the PCM encapsulation.

ACKNOWLEDGEMENT

The authors wish to thank Dr. Panniselvam from Department of Chemical Engineering RMIT University for his kind support in DSC scanning on samples of paraffin wax.

NOMENCLATURE

ρ	Density [kg/m^3]
ρ_0	Reference density [kg/m^3]
β	Thermal expansion [k^{-1}]
T_m	Melting temperature [^{o}C]
T_s	Solid temperature [^{o}C]
T_l	Liquid temperature [^{o}C]
g	Gravity [m/s^2]
μ	Dynamic viscosity [N s/m^2]
S_i	Momentum source term
h	Specific enthalpy [kJ/kg]
k	Thermal conductivity [W/m K]
h_s	Sensible enthalpy [J]
h_{ref}	Reference enthalpy [J]
C_p	Specific heat [J/ kg]
H	Total enthalpy [J]
L	Latent heat [J/kg]
γ	Liquid fraction
ε	Infinity avoidance constant
C	Morphology melting constant

REFERENCES

[1] Morisson, A.-K., 1978. Effect of phase-change energy storage on the performance of air-based and liquid-based solar heating sytems. *Solar Energy* 20: 57-67.

[2] Ghoneim, A.A., 1989. Comparison of theoretical models of phase-change and sensible heat storage for air and water-based solar heating systems. *Solar Energy* 42(3): 209-20.

[3] Evans, A.G., He, M.Y., Hutchinson, J.W., Shaw M., 2001. Temperature distribution in advanced power electronics systems nd the effect of phase change materials on temperature supprression during power pulses. *Journal of Electronic Packaging –Transactions of the ASME* 123: 211-217.

[4] Jegadheeswaram, S., and S.D. Pohekar. 2009. Performance enhancedment in latent heat thermal

storage system: A review. *Renewable and Sustainable Energy Reviews* 13: 2225-2244.

[5] Hasnain, S.M., 1998. Review on sustainable thermal storage technologies, Part 1: Heat storage materials and techniques. *Energy Conversion Management* 39: 1127-3-1138.

[6] Gharebagi, M., and I. Sezai. 1997. Enhancement of heat transfer in latent heat storage modules with internal fins. *Numerical Heat Transfer* Part A (53): 749-765.

[7] Lamberg, P., and K. Siren. 2004. Numerical and experimental investigation of melting and freezing processes in phase change material storage. *International Journal of Thermal Science* 43: 277-287.

[8] Jellouli, Y., Chouikh, R., Guizani, A., and Belghith, A., 2007. Numerical study of the moving boundary problem during melting process in a rectangular cavity heated from below. *American Journal Applied Science* 4: 251-256.

[9] Humphries, W.R., and E.I. Griggs., 1977. A design handbook for phase change thermal control and energy storage devices. NASA Technical Paper 1074, NASA Scientific and Technical Information Office.

[10] Reid, R., Prausnitz, J., and B. Poling. The Properties of Gases and Liquids. McGraw-Hill, New York.

[11] Shatikan, V., Ziskind, G., and R. Letan. 2005. Numerical investigation of a PCM-based heat sink with internal fins. *International Journal of Heat and Mass Transfe*r 48: 3689-3706.

[12] Brent, A.D., Voller, V.R., and K.J. Reid. 1988. Enthalpy-porosity technique for modeling convection-diffusion phase change: Application to the melting of a pure metal, *Numerical Heat Transfer* 13: 297-318.

[13] ANSYS Inc., ANSYS Fluent 12.0 User's Guide, 2009.